PRAMANA
— journal of
physics

Vol. 44, No. 4,
April 1995
pp. 375–391

Shape transitions in even Mo and Sm isotopes: Study in a new microscopic interacting boson model scheme

SUBRATA SARANGI and JITENDRA C PARIKH
Physical Research Laboratory, Navrangpura, Ahmedabad 380 009, India

MS received 21 February 1995

Abstract. A simple dynamic procedure, based on the deformed Hartree-Fock solution of a nucleus, is presented to construct the IBM operators in microscopic basis. The parameters of these operators are evaluated by establishing a Marumori mapping from the truncated shell model space onto the boson space. The transitions from spherical to axial-rotor shape observed in the low-lying levels of *even* $^{96-108}$Mo and $^{146-154}$Sm isotopes are reproduced qualitatively by applying this procedure with a fixed set of fermion input parameters to each chain. Variation of a few parameters in fermion space leads to quantitative agreement.

Keywords. Shape transitions; Mo and Sm isotopes; interacting boson model.

PACS Nos 21·60; 27·60

1. Introduction

The phenomenological interacting boson model (IBM) [1] has provided a unifying symmetry based scheme to study the low-energy collective behaviour of even-even medium and heavy mass nuclei and has been able to explain the observed collectivity very well [2, 3]. This success has quite naturally stimulated a great deal of endeavour to unravel the microscopic foundations of the model [4, 5]. Such calculations have been referred to as microscopic basis IBM calculations. It ought to be stressed that there is as yet no consensus among the scientists about the correct way to establish this connection. In this paper, we propose a different method and illustrate it with calculations of Mo and Sm isotopes.

In microscopic basis IBM calculations the construction of IBM operators is achieved in two stages: (i) An appropriate truncation of the large shell model space into a smaller space physically relevant to the low-lying spectra of interest; and (ii) Definition of the boson space and operators by establishing a correspondence with the truncated fermion space and operators defined therein.

Broadly speaking, two different procedures have emerged to carry out these operations. In the widely followed Otsuka–Arima–Iachello (OAI) mapping procedure [6–12] first a truncation of the many particle shell model space to the S-D or S-D-G subspace is carried out. The S-D-G subspace is composed of S, D and G pairs of identical particles corresponding to the pairing, quadrupole and hexadecapole collective degrees of freedom of the nucleus respectively. A Marumori mapping is then constructed from the S-D-G subspace onto the corresonding s-d-g boson space. The parameters of the n-body boson operators defined in th s-d-g space are then evaluated by equating them to the matrix elements of the corresponding n-body operators in the fermionic space. The recently suggested "democratic" mapping procedure [13, 14]

also follows a similar path. The procedures [15, 16] following the alternative Belyaev–Zelevinsky method first construct the boson operators and then carry out the truncation in the boson space.

In this paper, we describe a simple dynamic procedure [17] to construct the IBM operators from fermion basis and apply it to examine the collective shape transitions in even-A Mo and Sm isotopes. Taking into account the considerable amount of evidence that the G-pairs (or equivalently the g-bosons) play a necessary and sufficient role [10, 13, 16–23] in describing the low-lying spectra of interest, we assume that the relevant truncated fermion space is composed of only the "correlated" identical nucleon S, D and G pairs. Correspondingly we have the s-d-g IBM-2 boson space. We construct the correlated pairs by projecting good angular momentum states from mean field Hartree-Fock (HF) solutions. We then establish a Marumori mapping from the fermion single-pair and two-pair spaces to the corresponding one- and two- boson spaces. The boson matrix elements are then determined by equating them to the corresponding fermion matrix elements. Since a one-to-one correspondence from the identical two-pair space to the corres- ponding two boson space cannot be established, we ignore the identical boson interaction terms in the Hamiltonian. Actually, it has earlier been argued [4] that these terms do not play a significant role in the low-lying regions. The distinguishing aspect of our procedure from the OAI mapping is that in the latter N-pair states are mapped onto N-boson states and the fermion matrix elements are calculated in the N-pair space. Finally, due to lack of a suitable IBM-2 code incorporating g-bosons, the boson spectroscopic calculations are carried out in the IBM-1 domain by projecting from IBM-2 operators [24] and using the SDGIBM1 code of Devi and Kota [25].

The structure of the correlated identical nucleon pairs, which reflect the number of valence nucleons distributed over a set of single particle levels, the Pauli blocking effects etc., incorporates the dynamics and quite obviously plays a crucial role in evaluating the boson parameters. There have been several studies with varied approaches and approximations to study these aspects. The calculations [8, 9, 11] based on the broken pair approximation [26] evaluate the structure coefficients variationally with the assumption that the ground state of the nucleus consists of only S-pairs. These are clearly well-suited for spherical nuclei with a few valence nucleons. In the iterative scheme of Scholten [10] these coefficients are evaluated by minimising the N-pair ground state energy in the S-D-G space. This scheme has been applied to study the spherical to axially-deformed shape transition in the even-A Sm nuclei. There have also been procedures in the deformed basis where the coefficients are evaluated by projecting out good angular momentum states from deformed Cooper pairs obtained by number projection from BCS-Nilsson states [21, 22] or HFB solutions [20 27]. The correlated pairs constructed in our procedure from mean-field HF solutions do not include the pairing correlations, unlike those from the HFB solutions, but would include other deformation producing correlations, However, in the present study, we go beyond the work reported in [20, 27] in the sense that we actually construct the IBM Hamiltonian and other operators and carry out the spectroscopic calculations. Navrátil and Dobeš also evaluate these coefficients in the boson picture by establishing a canonical trans- formation from the non-collective boson space to the collective boson space and then choose the most collective state by looking at the lowest energy states of the Hamiltonian [16].

As mentioned earlier, we have applied our scheme to study the spherical to axial-rotor shape transition observed in the low-lying spectra of even $^{96-108}$Mo [28–30] and $^{146-154}$Sm [31, 32] isotopes. The microscopic IBM calculations for the

Mo isotopes are the first to be reported here. We compare our results for the Sm isotopes with those of Scholten [10] and Navrátil and Dobeš [16] who have also explicitly carried out the spectroscopic calculations using their respective procedures. From our results we observe the necessity to vary the strength parameters of the fermion two-body interaction (Surface delta interaction) in order to quantitatively reproduce the observed spectra and $B(E2)\uparrow$ values. Such variation in seen to be necessary in the transition region. Navrátil and Dobeš [16] have also observed the necessity to vary the fermion input parameters and have explicitly employed a thumb-rule (eq. (13) in ref. [16]) to vary them. Although no such variations were carried out by Scholten [10], the scaled-up spectra (with respect to the experimental ones) for the heavier Sm-chain probably indicate necessity of such a variation. We also observe similar effects in our results for Sm isotopic chain.

Our scheme of constructing the IBM operators is presented in § 2. The studies of shape transition in the Mo and Sm isotopic chains applying this scheme are presented in § 3. We summarize and conclude with a few remarks in § 4.

2. Our scheme

The scheme consists of four broad steps which are described in the following subsections. In the first step, we present a prescription to construct the correlated identical nucleon pairs from the occupied HF orbits of the nucleus. In § 2·2, we discuss the Marumori mapping from the correlated pair space onto the boson space. In § 2·3, we evaluate the IBM-2 parameters in terms of appropriate matrix elements in the fermion space. The IBM-1 parameters obtained from those of the IBM-2 operators by means of a projection scheme [24] are presented in § 2·4.

2.1 *Construction of correlated pairs*

We present here a simple prescription by which we construct the correlated pair states of identical nucleons for each nucleus. Clearly the structure of these pairs ought to effectively represent the distribution of all the valence nucleons ($\rho = \nu$(neutrons); π(protons)) over the chosen spherical model space $\{j_i^\rho\}$. A natural choice to carry out such a construction is to consider the occupancies of the spherical j_i^ρ orbits in a given state of the nucleus. However, a complete shell model calculation is almost impossible for the nuclei under our consideration. Hence we choose a practical, though approximate way out, i.e., to calculate the occupancies from the self-consistently generated set of deformed HF orbits. With the knowledge of the occupancies, we construct an effective single particle (s.p.) deformed orbit $|\rho; K\rangle_{\text{eff}}$ incorporating the relative distribution of the valence nucleons (ρ) over the model space. The correlated S, D, G pairs are then obtained by projecting out good angular momentum ($J = 0, 2, 4$ respectively) positive parity pairs from the two particle determinant defined by the states $|\rho; K\rangle_{\text{eff}}$.

We now describe the scheme in detail. We consider an even-even nucleus with n_ρ number of valence nucleons occupying a major oscillator shell $\{j_i^\rho\}$. The axially-deformed good-parity HF s.p. orbits $|\rho; \pm K\Pi\rangle$ for this system are then given by

$$|\rho; K\Pi\rangle = \sum_{j_i^\rho} C_{j_i^\rho K\Pi} |j_i^\rho K\Pi\rangle \quad \text{[time-like]} \tag{1}$$

$$|\rho; -K\Pi\rangle = \sum_{j_i^\rho} (-1)^{j_i^\rho - K} C_{j_i^\rho K\Pi} |j_i^\rho - K\Pi\rangle \quad \text{[time-reversed]} \tag{2}$$

where K and π are respectively, the s.p. projection (along the symmetry axis of the nucleus) and the parity associated with the orbit j_i^ρ. From the set of occupied HF we evaluate the occupancy of j_i^ρ

$$X_{j_i^\rho} = 2 \sum_{i=1}^{n_\rho/2} |C^{(l)}_{j_i^\rho}|^2 \tag{3}$$

where l is the index for the occupied orbits and the factor 2 accounts for the pair of time-like and time-reversed occupied orbits for each K and Π.

We then construct the effective s.p. deformed orbit

$$|\rho; K = \tfrac{1}{2}\rangle_{\text{eff}} = \sum_{j_i^\rho} p_{j_i^\rho} \bar{C}_{j_i^\rho} |j_i^\rho \tfrac{1}{2} \Pi\rangle. \tag{4}$$

Here the coefficients of expansion $\bar{C}_{j_i^\rho}$ are given by $\bar{C}_{j_i^\rho} = +\sqrt{X_{j_i^\rho}/n_\rho}$. The relative phase factors $p_{j_i^\rho}$ are fixed to be $p_{j_i^\rho} = C^{(1)}_{j_i^\rho} / |C^{(1)}_{j_i^\rho}|$ where $C^{(1)}_{j_i^\rho}$ are the coefficients of expansion of the first (energetically lowest) HF orbit. Note from the definition of $\bar{C}_{j_i^\rho}$ that this orbit is normalized.

A few points are to be noted at this step. The HF solutions for all the nuclei studied by us are prolate in nature. We therefore choose the projection quantum number $K = \frac{1}{2}$ for the effective orbit. This also allows all the spherical shells in the model space starting from $j^\rho = \frac{1}{2}$ to contribute to this orbit. Its constituent $\bar{C}_{j_i^\rho}$ coefficients retain the relative distribution of valence nucleons over the model space and the effects of Pauli blocking etc. The motivation behind the above choice of phases $p_{j_i^\rho}$ is the fact that the prolate orbit with this phase choice is invariably the most deformed orbit with maximum intrinsic quadrupole moment. One would therefore expect that the pair wave function constructed from such an effective orbit would describe the low-lying collective states of the nucleus. Moreover, as this orbit is defined over a major oscillator shell including the intruder shell, it does not have good parity. In case of an occupied intruder shell, there is also the question of defining the corresponding phase factor $p_{j_i^\rho}$ in (4). Since we finally consider only positive parity pair states projected out of the product of a pair of effective orbits, the phase of the intruder orbit here is irrelevant.

From the two particle determinant constructed by $|\rho; K = \pm 1/2\rangle_{\text{eff}}$, we project out the good angular momentum positive parity pairs $|B^\rho_{J M=0}\rangle$ or in short $|B^\rho_J\rangle$

$$|B^\rho_J\rangle = \sum_{kl} \mathscr{C}^\rho_{(kl)J} |(\rho; kl) J\rangle \tag{5}$$

where the expansion coefficients $\mathscr{C}^\rho_{(kl)J}$ is given by

$$\mathscr{C}^\rho_{(kl)J} = \mathscr{N}^\rho_J (-1)^{j_l^\rho - \frac{1}{2}} \sqrt{1+\delta_{kl}} (2 - \delta_{kl}) \langle j_k^\rho \tfrac{1}{2} j_l^\rho - \tfrac{1}{2} | j_k^\rho j_l^\rho : J0\rangle p_{j_k^\rho} p_{j_l^\rho} \bar{C}_{j_k^\rho} \bar{C}_{j_l^\rho}. \tag{6}$$

The quantity $\langle j_k^\rho \tfrac{1}{2} j_l^\rho - \tfrac{1}{2} | j_k^\rho j_l^\rho : J0\rangle$ in the above equation is the Clebsch–Gordan coefficient and $\mathscr{N}^\rho_J$ is the normalization factor. In (5) $|(\rho; kl) J\rangle = |(j_k^\rho j_l^\rho) J0\rangle$ is the two particle state coupled to angular momentum J. These correlated pairs are dynamic in nature, although in an average sense, as they are based on the occupancies of the model orbits calculated for each nucleus from the respective HF solutions. This prescription, like those of [20, 21, 22, 27], is applicable to all even-even nuclei—

spherical, transitional or rotational—away from closed-shell and whose lowest energy HF solution is prolate.

2.2 *Construction of the Boson operators*

Following usual tensor coupling notations, we may write the IBM-2 Hamiltonian

$$\mathscr{H}_{\text{IBM}-2} = \sum_J (-1)^J \varepsilon_J^\nu (b_J^{\nu\dagger} \cdot \tilde{b}_J^\nu) + \sum_J (-1)^J \varepsilon_J^\pi (b_J^{\pi\dagger} \cdot \tilde{b}_J^\pi) + \sum_{J_1 J_2 J_3 J_4; J'} (-1)^{J'} W_{J_1 J_2 J_3 J_4}^{J'} ((b_{J_1}^{\nu\dagger} \times b_{J_2}^{\pi\dagger})^{J'} \cdot (\tilde{b}_{J_3}^\nu \times \tilde{b}_{J_4}^\pi)^{J'}) \tag{7}$$

where $b_J^{\rho\dagger}$ and $\tilde{b}_J^\rho$ are respectively the boson creation and annihilation spherical tensor operators with $J = 0, 2$ and 4 for the s, d and g bosons. We also have the $E2$-transition operator

$$\mathscr{T}_{\text{IBM}-2}^{(\text{E2})} = \sum_{\rho=\nu,\pi} \sum_{JJ'} e_{JJ'}^\rho (b_J^{\rho\dagger} \tilde{b}_{J'}^\rho)_0^2. \tag{8}$$

Our objective is to evaluate the single boson energy ε_J^ρ, the $\nu - \pi$ boson two-body matrix element (tbme) $W_{J_1 J_2 J_3 J_4}^{J'}$ in eq. (7) and the effective boson charge $e_{JJ'}^\rho$ in eq. (8) microscopically. To this end, we first establish the following Marumori mapping from the identical nucleon pair space onto the boson space

nucleon pairs bosons

$$|B_J^\rho\rangle \rightarrow |b_J^\rho\rangle;\ J = 0, 2, 4 \tag{9}$$

$$|(B_{J_1}^\nu B_{J_2}^\pi) J\rangle \rightarrow |(b_{J_1}^\nu b_{J_2}^\pi) J\rangle;\ J_1, J_2 = 0, 2, 4. \tag{10}$$

It is to be noted in (10) that the nucleon pairs and the bosons being distinguishable, there is no (anti) symmetry requirement and the one-to-one correspondence is straightforward.

The above mappings (9–10) lead to evaluation of the parameters of the boson operators in eqs (7–8) in the following manner

boson matrix elements nucleon pair matrix elements

$$\varepsilon_J^\rho \equiv \langle b_J^\rho | \mathscr{H}_{\text{IBM}-2} | b_J^\rho \rangle = \langle B_J^\rho | \mathscr{H}_\rho | B_J^\rho \rangle \tag{11}$$

$$W_{J_1 J_2 J_3 J_4}^J \equiv \langle (b_{J_1}^\nu b_{J_2}^\pi) J | \mathscr{H}_{\text{IBM}-2} | (b_{J_3}^\nu b_{J_4}^\pi) J \rangle = \langle (B_{J_1}^\nu B_{J_2}^\pi) J | \mathscr{V}_{\nu\pi}^F | (B_{J_3}^\nu B_{J_4}^\pi) J \rangle \tag{12}$$

$$e_{JJ'}^\rho \equiv \langle b_J^\rho | \mathscr{T}_{\text{IBM}-2}^{(\text{E2})} | b_{J'}^\rho \rangle = \langle B_J^\rho | \mathscr{T}^{(\text{E2})} | B_J^\rho \rangle. \tag{13}$$

On the r.h.s. of eqs (11–13), we have respectively the one-plus-two-body identical nucleon Hamiltonian $\mathscr{H}_\rho$, the two-body neutron-proton interaction operator $\mathscr{V}_{\nu\pi}$ and the fermion $E2$-transition operator $\mathscr{T}^{(\text{E2})}$ discussed in the next subsection.

As pointed out earlier, a one-to-one correspondence between the states $|(B_{J_1}^\rho B_{J_2}^\rho) J\rangle$ and $|(b_{J_1}^\rho b_{J_2}^\rho) J\rangle$ cannot be established. We have, therefore, dropped the terms involving these boson states in the Hamiltonian $\mathscr{H}_{\text{IBM}-2}$ (eq. (7)). However, this approximation is not a severe handicap as it has been shown [4] that in the low-lying spectra these matrix elements play a negligible role.

Further, the Marumori mapping constructed in (9–10) are not of OAI type where N-pair ($N = N_\nu + N_\pi$) states are mapped onto N-boson states [6–12] and the boson parameters are evaluated by calculating a few fermion matrix elements in the N-pair space using the generalised seniority scheme.

2.3 *Evaluation of the boson parameters*

2.3.1 *The single boson energy*: The single boson energy $e^\rho_J = \langle B^\rho_J | \mathscr{H}_\rho | B^\rho_J \rangle$ of (11) alongwith (5) for $|B^\rho_J\rangle$ is given by

$$\varepsilon^\rho_J = \sum_{k_1 l_2} \sum_{k_2 l_2} \mathscr{C}^{\rho}_{(k_1 l_1) J} \mathscr{C}^{\rho}_{(k_2 l_2) J} \langle (\rho; k_1 l_1) J | \mathscr{H}_\rho | (\rho; k_2 l_2) J \rangle. \tag{14}$$

The matrix elements (m.e.) on the r.h.s. of (14) is easily evaluated

$$\langle (\rho; k_1 l_1) J | \mathscr{H}_\rho | (\rho; k_2 l_2) J \rangle = (\varepsilon_{j^\rho_{k_1}} + \varepsilon_{j^\rho_{l_1}}) \delta_{j^\rho_{k_1} j^\rho_{k_2}} \delta_{j^\rho_{l_1} j^\rho_{l_2}} + V^J_{j^\rho_{k_1} j^\rho_{l_1} j^\rho_{k_2} j^\rho_{l_2}} \tag{15}$$

where $\varepsilon_{j^\rho_k}$ is the single particle energy (spe) of the valence SM orbits j^ρ_k and $V^J_{j^\rho_{k_1} j^\rho_{l_1} j^\rho_{k_2} j^\rho_{l_2}}$ is the identical particle nucleonic two-body matrix element (tbme)

2.3.2 *The neutron-proton boson interaction matrix element*: The ν–π boson two-body matrix element $W^J_{J_1 J_2 J_3 J_4} = \langle (B^\nu_{J_1} B^\pi_{J_2}) J | \mathscr{V}_{\nu\pi} | (B^\nu_{J_3} B^\pi_{J_4}) J \rangle$ of (12) alongwith (5) is given by

$$W^J_{J_1 J_2 J_3 J_4} = \sum_{k_1 l_1} \sum_{k_2 l_2} \sum_{k_3 l_3} \sum_{k_4 l_4} \mathscr{C}^{\nu}_{(k_1 l_1) J_1} \mathscr{C}^{\pi}_{(k_2 l_2) J_2} \mathscr{C}^{\nu}_{(k_3 l_3) J_3} \mathscr{C}^{\pi}_{(k_4 l_4) J_4}$$
$$\langle ((\nu; k_1 l_1) J_1, (\pi; k_2 l_2) J_2) J | \mathscr{V}_{\nu\pi} | ((\nu; k_3 l_3) J_3, (\pi; k_4 l_4) J_4) J \rangle. \tag{16}$$

The matrix element on the rhs of (16) is the basic matrix element with the two-body ν–π-interaction operator

$$V_{\nu\pi} = \sum_{j^\nu j^\pi j'^\nu j'^\pi; J'} [J']^{1/2} V^{J'}_{j^\nu j^\pi j'^\nu j'^\pi} ((a^\dagger_{j^\nu} \times a^\dagger_{j^\pi})^{J'} \times (\tilde{a}_{j'^\nu} \times \tilde{a}_{j'^\pi})^{J'})^0 \tag{17}$$

with $a^\dagger_{j^\rho}, \tilde{a}_{j^\rho}$ etc. as the nucleon creation and annihilation tensor operators and the matrix elements $V^{J'}_{j^\nu j^\pi j'^\nu j'^\pi}$ in ν–π formalism.

Rewriting the operator $\mathscr{V}_{\nu\pi}$ in the multipole form and applying the Wigner–Eckart theorem, the basic matrix element can be factorised [33]

$$\langle ((\nu; k_1 l_1) J_1, (\pi; k_2 l_2) J_2) J | \mathscr{V}_{\nu\pi} | ((\nu; k_3 l_3) J_3), (\pi; k_4 l_4) J_4) J \rangle$$
$$= (-1)^{J_2 + J_3 + J} \sum_{j^\nu j^\pi j'^\nu j'^\pi; J'} (-1)^{j^\pi + j'^\nu + J'} [J'] V^{J'}_{j^\nu j^\pi j'^\nu j'^\pi}$$
$$\sum_{J''} \begin{Bmatrix} J_1 & J_2 & J \\ J_4 & J_3 & J'' \end{Bmatrix} \begin{Bmatrix} j^\nu & j^\pi & J' \\ j'^\pi & j'^\nu & J'' \end{Bmatrix} \langle (\nu; k_1 l_1) J_1 \| (a^\dagger_{j^\pi} \times \tilde{a}_{j'^\nu})^{J''} \| (\nu; k_3 l_3) J_3 \rangle$$
$$\langle (\pi; k_2 l_2) J_2 \| (a^\dagger_{j^\pi} \times \tilde{a}_{j'^\pi})^{J''} \| (\pi; k_4 l_4) J_4 \rangle. \tag{18}$$

The m.e.'s on the rhs of (18) are evaluated by employing standard techniques of shell model spectroscopy, namely, intermediate state expansion, recoupling of spherical

tensors and application of the fermion anti-commutation relations. We obtain

$$\langle((\nu;k_1l_1)J_1,(\pi;k_2l_2)J_2)J|\mathscr{V}_{\nu\pi}|((\nu;k_3l_3)J_3,(\pi;k_4l_4)J_4)J\rangle$$

$$= (-1)^{J_1+J_4+J+1}\prod_{i=1}^{4}\zeta_{k_il_i}[J_i]^{1/2}\varepsilon_{k_il_iJ_i}$$

$$\sum_{J'J''}(-1)^{j^\nu_{k_1}+j^\nu_{k_3}+j^\nu_{l_1}+j^\pi_{l_2}+J'}[J'J'']\,V^{J'}_{j^\nu_{k_1}j^\pi_{k_2}j^\nu_{k_3}j^\pi_{k_4}}\begin{Bmatrix}J_1 & J_2 & J\\ J_4 & J_3 & J''\end{Bmatrix}$$

$$\begin{Bmatrix}j^\nu_{k_1} & j^\pi_{k_2} & J'\\ j^\pi_{k_4} & j^\nu_{k_3} & J''\end{Bmatrix}\begin{Bmatrix}J_1 & j^\nu_{k_1} & j^\nu_{l_1}\\ j^\nu_{k_3} & J_3 & J''\end{Bmatrix}\begin{Bmatrix}J_2 & j^\pi_{k_2} & j^\pi_{l_2}\\ j^\pi_{k_4} & J_4 & J''\end{Bmatrix}\delta_{j^\nu_{l_1}j^\nu_{l_3}}\delta_{j^\pi_{l_2}j^\pi_{l_4}} \tag{19}$$

where $\zeta_{k_il_i}=(1/(1+\delta_{k_il_i})^{1/2})$, $[J]=2J+1$ and the exchange operator ε_{klJ} defined as

$$\varepsilon_{klJ}f(k,l,J)=f(k,l,J)-(-1)^{j_k+j_l-J}f(l,k,J). \tag{20}$$

2.3.3 *The E2-transition effective boson charge*: The effective boson charge $e^\rho_{JJ'}$ for $E2$-transition in (8) is evaluated from (13). By applying Wigner–Eckart theorem and carrying out the contraction on the double-barred matrix element through boson commutation relations, the boson matrix element on the lhs of (13) can be reduced to

$$\langle b^\rho_{J_1}|\mathscr{T}^{(E2)}_{IBM-2}|b^\rho_{J_2}\rangle=\frac{[2]^{1/2}}{[J_1]^{1/2}}\langle J_2020|J_10\rangle e^\rho_{J_1J_2} \tag{21}$$

where the quantity $\langle J_2020|J_10\rangle$ is the Clebsch–Gordan coefficient. The effective charge parameter of the bosons is thus given by

$$e^\rho_{J_1J_2}=\frac{[J_1]^{1/2}\langle B^\rho_{J_1}|\mathscr{T}^{(E2)}|B^\rho_{J_2}\rangle}{[2]^{1/2}\langle J_2020|J_10\rangle}. \tag{22}$$

The $E2$-transition operator $\mathscr{T}^{(E2)}$ in the nucleonic space is given by

$$\mathscr{T}^{(E2)}=-\frac{1}{\sqrt{5}}\sum_\rho e_\rho\sum_{j^\rho j'^\rho}q_{j^\rho j'^\rho}(a^\dagger_{j^\rho}\times\tilde{a}_{j'^\rho})^2_0 \tag{23}$$

where e_ρ is the effective nucleon charge, $q_{j^\rho j'^\rho}=\langle j^\rho\|r^2\,Y^2\|j'^\rho\rangle$ is the reduced quadrupole matrix element in units of oscillator size parameter $b^2_\rho(=0{\cdot}0102(4N_\rho/A^2)^{-1/3}$ barns) [34] for a nucleus with N_ρ number of ρ-pairs and atomic number A.

Expanding the m.e. on the rhs of (22) by (5) we have

$$\langle B^\rho_{J_1}|\mathscr{T}^{(E2)}|B^\rho_{J_2}\rangle=\sum_{k_1l_1}\sum_{k_2l_2}\mathscr{C}^\rho_{(k_1l_1)J_1}\mathscr{C}^\rho_{(k_2l_2)J_2}\langle(\rho;k_1l_1)J_1|\mathscr{T}^{(E2)}|(\rho;k_2l_2)J_2\rangle. \tag{24}$$

The basic matrix element on the rhs of (24) is evaluated by substituting for $\mathscr{T}^{(E2)}$ (23) and applying the spherical tensor recoupling and commutation relations. We obtain

$$\langle(\rho;k_1l_1)J_1|\mathscr{T}^{(E2)}|(\rho;k_2l_2)J_2\rangle$$

$$=e_\rho[J_2]^{1/2}\langle J_2020|J_10\rangle\varepsilon_{k_1l_1J_1}\varepsilon_{k_2l_2J_2}(-1)^{j^\rho_{k_1}+j^\rho_{l_1}+J_2}q_{j^\rho_{k_1}j^\rho_{k_2}}$$

$$\zeta_{k_1l_1}\zeta_{k_2l_2}\begin{Bmatrix}j^\rho_{k_1} & j^\rho_{l_1} & J_1\\ J_2 & 2 & j^\rho_{k_2}\end{Bmatrix}\delta_{j^\rho_{l_1}j^\rho_{l_2}} \tag{25}$$

Combining (22), (24) and (25) we calculate the effective charge parameter $\varepsilon^{\rho}_{J_1J_2}$.

2.3 *Construction of IBM-1 operators*

Due to the lack of an IBM-2 code incorporating g-bosons explicitly, we carry out the spectroscopic calculations in IBM-1 regime. The parameters of the IBM-1 operators are calculated from those of IBM-2 by a projection scheme [24] based on the F-spin symmetry amongst neutron and proton bosons. The IBM-2 to IBM-1 projection is carried out with the assumption that the low-lying IBM-2 levels of our interest have F-spin $F = F_{\max}$ and hence are completely symmetric under interchange of ν–π labels. This symmetry can be realized by either constructing an F-scalar Hamiltonian [35] or, alternatively, by including in a non-F-scalar Hamiltonian a large Majorana force $M_{\nu\pi}$ [36, 37].

The IBM-2 Hamiltonian (eq. (7)) constructed in our microscopic procedure is clearly not F-scalar. However, we assume that the low-lying levels and, in particular, the Yrast levels among them that we are interested in do have $F = F_{\max}$ and project out the IBM-1 Hamiltonian from the IBM-2 Hamiltonian. Those terms in the expansion of the IBM-2 Hamiltonian which contribute to the Majorana operator collapse in IBM-1 because of symmetry requirements of the IBM-1 states. Out of the 82 parameters in the two-body part of $\mathscr{H}_{\text{IBM}-2}$ only 68 contribute to $\mathscr{H}_{\text{IBM}-1}$ m.e. and the rest are mapped to zero. The 3 single boson energies ε_J and 32 two-body matrix elements $V^{J'}_{J_1J_2J_3J_4}$ of the (sdg) IBM-1 Hamiltonian

$$\mathscr{H}_{\text{IBM}-1} = \sum_J (-1)^J \varepsilon_J (b^{\dagger}_J \cdot \tilde{b}_J) + \sum_{J_1J_2J_3J_4;J'} (-1)^{J'} \zeta_{J_1J_2}\zeta_{J_3J_4} V^{J'}_{J_1J_2J_3J_4} (b^{\dagger}_{J_1} b^{\dagger}_{J_2})^{J'} \cdot (\tilde{b}_{J_3}\tilde{b}_{J_4})^{J'} \tag{26}$$

and the 4 effective $E2$-charge parameters $e_{JJ'}$ of the IBM-1 $E2$-transition operator

$$\mathscr{T}^{(E2)}_{\text{IBM}-2} = \sum_{JJ'} e_{JJ'} (b^{\dagger}_J \tilde{b}'_J)^2_0 \tag{27}$$

are related to the corresponding IBM-2 parameters through the neutron(proton) boson numbers $N_\nu(N_\pi)$ and the total boson number N and are given below

IBM − 1 IBM − 2

$$\varepsilon_J = \frac{1}{N}(N_\nu \varepsilon^{\nu}_J + N_\pi \varepsilon^{\pi}_J) \tag{28}$$

$$V^{J'}_{J_1J_2J_3J_4} = \frac{N_\nu N_\pi}{N(N-1)} \bar{W}^{J'}_{J_1J_2J_3J_4} \tag{29}$$

$$e_{JJ'} = \frac{1}{N}(N_\nu e^{\nu}_{JJ'} + N_\pi e^{\pi}_{JJ'}). \tag{30}$$

In eq. (29) $\bar{W}^{J'}_{J_1J_2J_3J_4}$ is the sum of all $W^{J'}_{J_1J_2J_3J_4}$ for a given J' in $\mathscr{H}_{\text{IBM}-2}$ including the distinct permutations of (J_1, J_2) and (J_3, J_4) respectively.

The IBM-1 parameters (28–30) are then used in the SDGIBM-1 boson code of Devi and Kota [25] to produce the spectra and $B(E2)$ values for the even-even Mo and Sm isotopes. Due to computational difficulties we have truncated the boson space to

configurations with number of g-bosons $N_g \leqslant 2$ for all calculations reported here. In case of the Sm isotopes, the basis space has been further truncated by imposing the condition on number of s-bosons $N_s \geqslant 2$ on the basis states. Earlier calculations [16, 38] have demonstrated that such approximations produce satisfactory results.

3. Shape transition in Mo and Sm isotopes

We now present the results of the application of this simple procedure to study the spherical to axially-deformed shape transition in even—A^{96-108}Mo and $^{146-154}$Sm isotopes. We have used the surface delta interaction (SDI) $\mathcal{O}_{\rho\rho'}$ as the residual two-body interaction. It can be written in terms of spherical harmonics Y^l_m

$$\mathcal{O}_{\rho\rho'} = -A_{\rho\rho'} \sum_{l=0}^{\infty} (-1)^l (2l+1)^{1/2} (Y^l(\rho) \cdot Y^l(\rho')) \tag{31}$$

with strength parameters $A_{\rho\rho'}$. Qualtitative features of shape transition are observed with a given set of fermion input parameters, namely, spe $\varepsilon_{j\rho}$, SDI strength $A_{\rho\rho'}$ and effective nucleon charge e_ρ, for each set of isotopes. However, in quantitative terms, the same set of parameters while producing results in agreement with experiment for the lighter isotopes, produce scaled-up spectra for the heavier ones. One then needs to vary these parameters in the deformed region to reproduce numbers akin to experimental results. Such scaling-up of spectra has also been reported by other authors [10, 12, 16]. Navrátil and Dobesy carry out the variation of all the input parameters dynamically by a further parametrization [16] involving the boson numbers of the nucleus under consideration. Our attempt, however, has been to minimize the number of free parameters and also to economise on their variation.In order to demonstrate the necessity of varying these parameters, we adopt the following approach. For the Mo chain, we carry out variation of $A_{\rho\rho'}$ with a view to closely reproducing the experimental results. For the Sm chain, however, we keep the strength parameters fixed and compare the results with the observed spectra as well as with those of Scholten [10] whose calculations are also carried out without variation of the parameters. The effective nucleon charges for the Sm isotopes are varied to compare with the results of Navrátil and Dobesy [16]. We have also carried out detailed calculations for ^{148}Sm and ^{152}Sm with different values of the parameters $A_{\rho\rho'}$ and e_ρ. Results of these calculations are not given here for brevity but they compare well with those of [16, 38, 39] and experiments [31, 32].

3.1 *The Mo isotopes*

The model spaces for the valence protons and neutrons in the even $^{96-108}$Mo isotopes alongwith the spe [40] are given in table 1. It has also been shown [40] that the role of the $2p_{1/2}$ shell protons is negligible in the shape transition; hence we ignore them. The set of SDI strength parameters $A_{\nu\nu} = A_{\pi\pi} = 0{\cdot}35$ MeV and $A_{\nu\pi} = 0{\cdot}6$ MeV, taken by Federman and Pittel [41] to study the shape transitions in this isotopic chain, produce in our calculations results in agreement with experiment for the lighter isotopes but scaled-up spectra for the heavier ones. We, therefore, vary these parameters as shown in table 2. These numbers indicate, as one would expect, that the deformation producing $\nu\pi$ interaction becomes much stronger in the deformed heavy isotopes compared to the identical particle interaction which would include the

Table 1. The model space and the single particle energies for Mo isotopes.

	orbit	energy (MeV)
protons	$1g_{9/2}$	0·0
neutrons	$2d_{5/2}$	0·0
	$3s_{1/2}$	1·0
	$2d_{3/2}$	2·5
	$1g_{7/2}$	3·0
	$1h_{11/2}$	3·6

Table 2. Adopted SDI strength parameters for $^{96-108}$Mo isotopes.

Isotope	$A_{\rho\rho}(\rho = \nu, \pi)$ (in MeV)	$A_{\nu\pi}$ (in MeV)
^{96}Mo	0·37	0·60
^{98}Mo	0·37	0·60
^{100}Mo	0·33	0·60
^{102}Mo	0·10	0·40
^{104}Mo	0·05	0·40
^{106}Mo	0·05	0·40
^{108}Mo	0·05	0·40

sphericity producing pairing interactions even though their absolute values decrease. The effective neutron charges are chosen to be $e_\nu = 0{\cdot}9e$ and $e_\pi = 1{\cdot}9e$.

In the axially-deformed prolate HF solutions we do not observe occupation of the intruder $1h_{11/2}$ orbit. The normalized occupancies $|\bar{C}_{j^\nu}|^2$ calculated from $|\nu; k = 1/2)_{\text{eff}}$ (4) for every valence orbit j_i^ν are plotted for all isotopes in figure 1(a). In the case of ^{98}Mo the $2d_{5/2}$ orbit gets almost filled with very little participation of the rest of the model orbits and we observe a (sub)shell effect here. It has been argued [42] that this effect at $N = 56$, 58 is responsible for the delay in the onset of shape transition in Mo isotopes. With addition of more neutrons, collectivity sets in and for $A = 106$, 108 the $2d_{3/2}$ and $1g_{7/2}$ orbits also take part substantially.

Federman and Pittel [43], in their analysis of the microscopic aspects of nuclear deformation and shape transition, proposed that the onset of nuclear deformation occurs in the region where valence neutrons and protons occupy spherical orbits with good overlap. The neutron and proton orbits $(n_\nu l_\nu j_\nu)$ and $(n_\pi l_\pi j_\pi)$ are shown to have good overlap [44] if $n_\nu = n_\pi$ and $l_\nu = l_\pi$, $l_\pi \pm 1$. Following this, Federman and Pittel [41] showed that it is indeed the occupation of the $(1g_{9/2})^\pi$ and $(1g_{7/2})^\nu$ orbits by the valence nucleons which is responsible for the onset of deformation in the heavier Mo isotopes. In figure 1(a), we observe similar effects with $1g_{7/2}$ being rapidly occupied for $A = 104$–108. Similar effects are also seen in the occupancies of the model orbits for the Sm isotopes.

The IBM-1 d- and g-boson energies $\varepsilon_d, \varepsilon_g$ with respect to the s-boson energies are plotted in figure 1(b). Barring the case of ^{98}Mo, these quantities vary smoothly. It

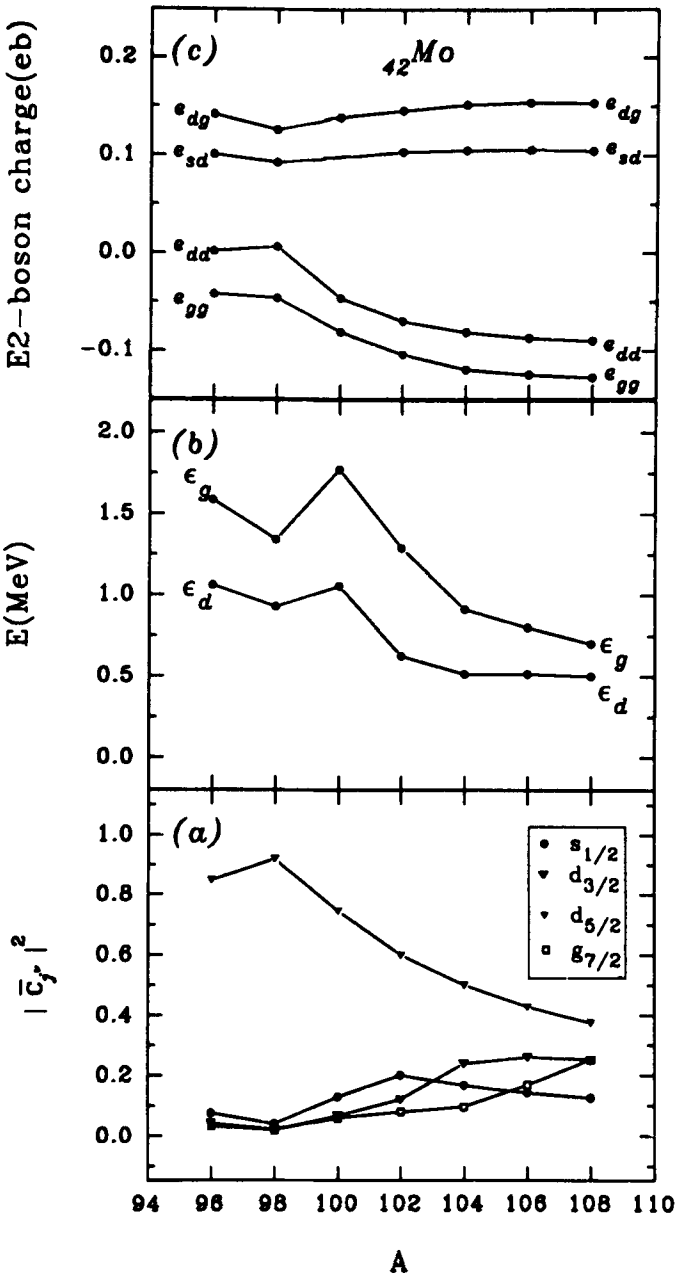

Figure 1. Mo Isotopes: (a) effective occupancies $|\bar{C}_{j^\nu}|^2$ of single particle neutron orbits from $|\nu; k = +\frac{1}{2}\rangle_{eff}$ orbit; (b) the IBM-1 d- and g- boson energies ε_d and ε_g w.r.t ε_s; and (c) IBM-1 effective boson charges for $E2$-transitions are plotted against the atomic number A.

should be noted that for $^{104-108}$Mo, with the SDI strength parameters kept constant table 2, there is a gradual decrease in the ε_d–ε_g gap. This decrease facilitates a stronger mixing of the d- and g-bosons and probably helps the onset and sustenance of the deformation.

The IBM-1 $E2$-charges $e_{JJ'}$ in eb unit are plotted in figure 1(c). It is gratifying to note that for the heavier (deformed) nuclei these microscopically calculated parameters have the same relative phases as the $E2$-transition operator in $SU(3)$ limit [45]

$$\mathscr{T}^{(E2)}_{IBM-1}(SU(3) = e^B\left(4\left(\frac{7}{15}\right)^{1/2}(s^\dagger\tilde{d} + d^\dagger\tilde{s})^2_0 - 11\left(\frac{2}{27}\right)^{1/2}(d^\dagger\tilde{d})^2_0 + \frac{36}{\sqrt{105}}(d^\dagger\tilde{g} + g^\dagger\tilde{d})^2_0 - 2\left(\frac{33}{7}\right)^{1/2}(g^\dagger\tilde{g})^2_0\right) \tag{32}$$

and with the free parameter $e^B = 0{\cdot}04$ eb, the two sets of parameters become comparable for the deformed nuclei like $^{106-108}$Mo.

In figure 2(a), the observed [31] and calculated 2^+_1, 4^+_1 and 6^+_1 energies of the isotopes (A) are plotted with respect to the respective ground state energies. The

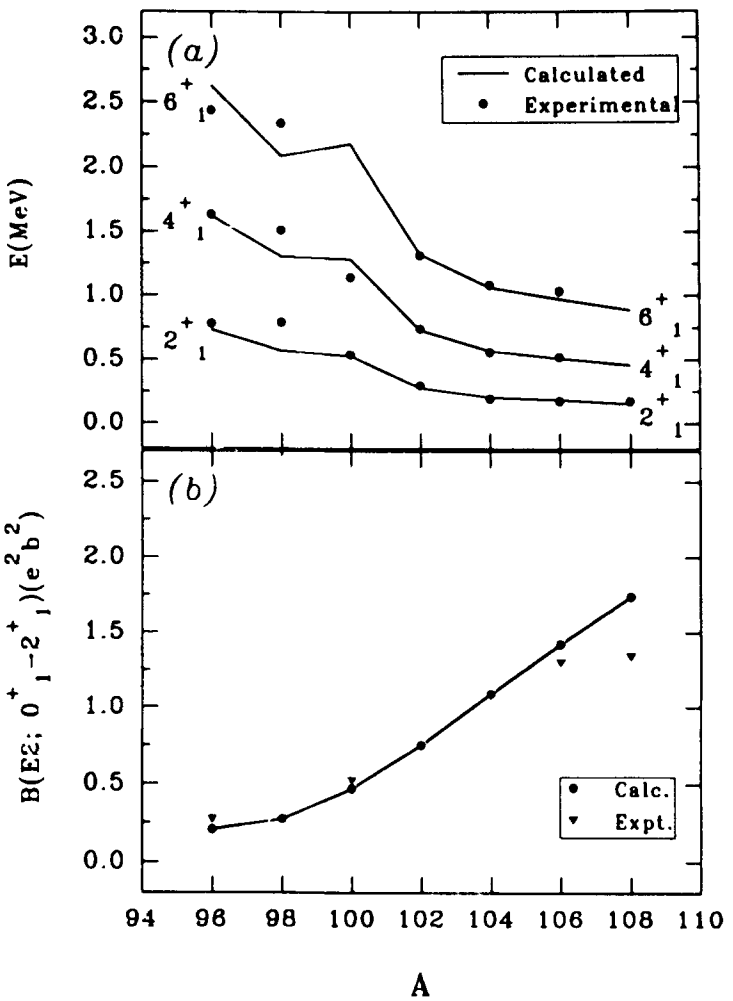

Figure 2. Mo isotopes: the experimental and calculated (**a**) Yrast spectra; and (**b**) the $E2$-transition probabilities ($B(E2; 0^+_1 \to 2^+_1)$).

$B(E2; 0_1^+ \rightarrow 2_1^+)$ (or $B(E2)\uparrow$) are presented alongwith the experimental values [32] in figure 2(b). The spherical to axial-rotor shape transition is clearly borne out with lowering of the 2_1^+ level with A, the transition in the energy spectrum from vibrational to rotational and also the enhancement of $B(E2)\uparrow$ values around $A = 100, 102$. The overproduction of $B(E2)\uparrow$ for $A = 106, 108$ is also observed by other phenomenological studies [30, 36]. It may be noted in table 2 that the necessity to vary the SDI strength parameters occurs near $A \simeq 100, 102$ where the transition evidently occurs.

3.2 *The Sm isotopes*

The single particle spaces and the corresponding energies of the orbits are given in table 3. The beginning-shell single-particle (BSSP) energies [7] have been taken for both neutrons and protons. The strength parameters of SDI are kept fixed at $A_{\nu\nu} = A_{\pi\pi} = 0{\cdot}3$ MeV and $A_{\nu\pi} = 0{\cdot}12$ MeV. The energies of a few low-lying levels with respect to the corresponding ground state energies given by our calculation alongwith the corresponding experimental values [31] are plotted in figure 3(a). The spectra generated in [10] are plotted in figure 3(b) for comparison. The calculated levels for the deformed nuclei, namely, $^{152-154}$Sm are pushed up compared to the observed ones. The same effects are also observed in figure 3(b). The evidence of the shape transition at $A = 150$–152 is clearly seen from the Yrast levels 2_1^+ and 4_1^+ plotted with respect to the ground state. The behavior of the 0_2^+ has been pointed out to be remarkable [47] in the shape transition. Being a member of the two-phonon triplet of a spherical nucleus, it first drops linearly alongwith 2_2^+ and 4_1^+. As the transition to axially-deformed shape occurs, it moves up and becomes the head of the β-band. The 2_2^+ level also goes up as seen in the experimental curve (figure 3(a)). However, the 0_2^+ and 2_2^+ levels for $^{152-154}$Sm in our calculation are produced at higher energies compared to those of [10] in figure 3(b). As already mentioned earlier, the excess of pairing correlation supplied by a higher than realistic value of $A_{\nu\nu}$ and $A_{\pi\pi}$ may be playing a role in this scale-up. It is also likely that the excited boson states such as s′ and d′ play a role even in the low-lying spectra of deformed nuclei. In addition, for our calculated levels the mixing of F-spin mixed-symmetry states with those of F-spin symmetric ones may also be party responsible. As Scholten's calculations are carried out in IBM-2 with a Majorana force which pushes the F-spin mixed-symmetry levels up, the 0_2^+, 2_2^+ levels produced thereby should correspond closer to pure F-spin symmetric levels.

Table 3. The neutron and proton model spaces for $^{146-156}$Sm and the spe.

Neutrons		Protons	
orbits	energies (MeV)	orbits	energies (MeV)
$2f_{7/2}$	1·00	$1g_{7/2}$	0·00
$3p_{3/2}$	1·50	$2d_{5/2}$	0·96
$3p_{1/2}$	2·25	$2d_{3/2}$	2·69
$1h_{9/2}$	2·45	$1h_{11/2}$	2·76
$2f_{5/2}$	2·60	$3s_{1/2}$	2·99
$1i_{13/2}$	2·80	—	—

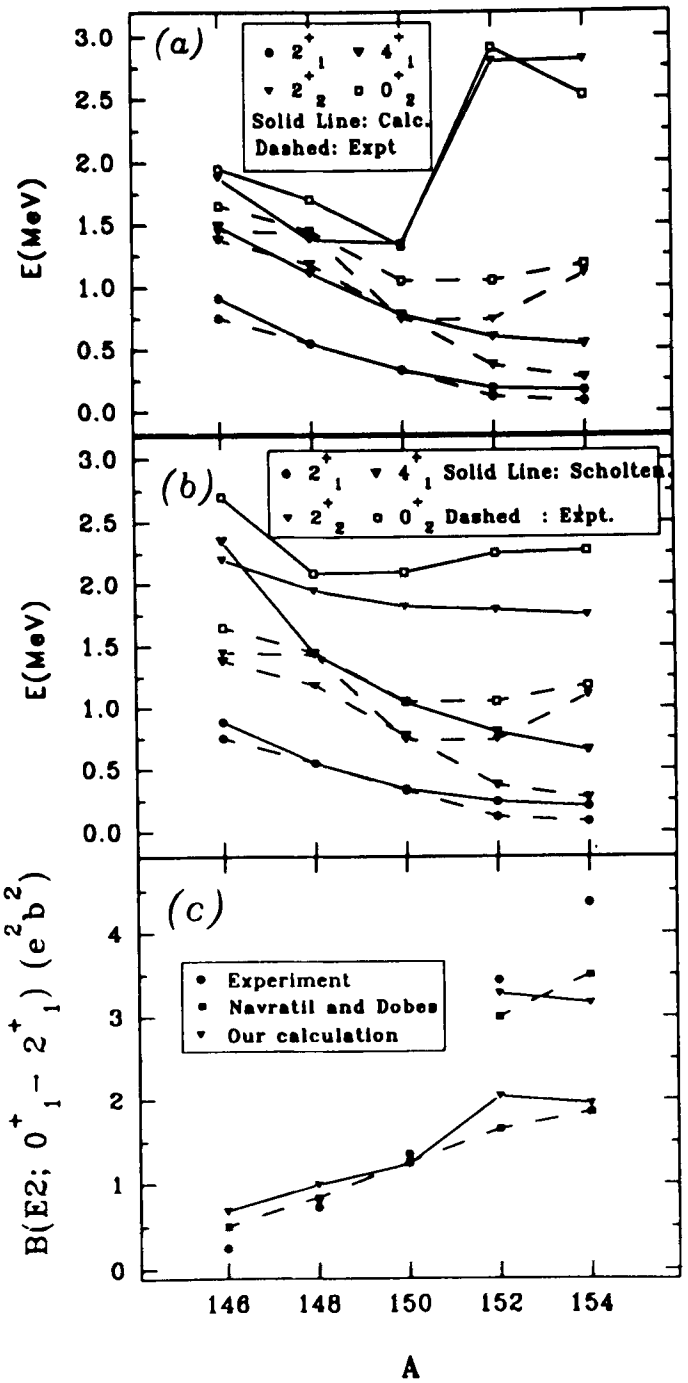

Figure 3. Sm isotopes: (a) experimental (expt.) and calculated (calc). spectra; (b) spectra produced in Scholten's calculation alongwith the experiment levels; and (c) the $B(E2;0_1^+ \rightarrow 2_1^+)$ in e^2b^2 units. A different set of e_ν and e_π produces the $B(E2)$ values closer to the experimental values for $A = 152, 154$.

The $B(E2)\uparrow$ values plotted in figure 2(c) alongwith the experimental values [32] and those of Navrátil and Dobesy [16] also show the enhancement at $A \simeq 152$—a characteristic of the transition. However, we observe that the initial choice of the fermion effective charges $e_\nu = 0{\cdot}5\,e$ and $e_\pi = 1{\cdot}3\,e$ is not able to produce enough enhancement as observed at the transition. In order to reproduce the enhancement closer to observed values we have to adopt a new set of parameters, i.e. $e_\nu = 0{\cdot}7$ e and $e_\pi = 1{\cdot}6$ e. Similar observation has also been made by Navrátil and Dobesy. Such a variation of the parameters is also evidently necessary in the case of the spectra (both ours as well as Scholten's) which while qualitatively showing the transition are scaled up at the point of transition, i.e. at $A = 150$–152.

4. Discussion

A great deal of work probing the microscopic foundations of IBM has been reported in literature. Several schemes and procedures have been developed to construct the bosons and the bosonic operators microscopically from fermion inputs. These studies demonstrate various degrees of success in explaining different aspects of low-lying collectivity in nuclei. However, there have been only very few microscopic IBM calculations to study detailed spectroscopic properties.

The highlight of the procedure presented here is that with a simple prescription it dynamically evaluates the boson structure and matrix elements of the boson operators for each nucleus from its deformed HF solution. Secondly, this procedure is success- fully applied to carry out spectroscopic calculations to study the spherical to axially- deformed shape transition in even-A Mo and Sm isotopes.

This procedure is based on the following assumptions:

(i) The truncation of the full shell model space to S-D-G space is both viable and sufficient;
(ii) The many particle fermion states of the S-D-G space and the matrix elements of the fermionic operators defined in this space are correctly represented by the corresponding boson states in the s-d-g space and the matrix elements of the bosonic operators;
(iii) The lowest energy HF solutions from which the correlated S, D and G pairs are constructed are prolate in character.
(iv) The identical boson interaction terms are negligible compared to the neutron-proton interaction term in the boson Hamiltonian.
(v) The low-lying IBM-2 states of interest are F-spin symmetric.
(vi) For computational limitations, the boson configuration space has been truncated with the condition $N_g \leqslant 2$ of g-bosons. For the Sm isotpoes, we also have a further truncation $N_s \geqslant 2$ of s-bosons.

In our study of shape transitions, we observe a necessity to vary the fermion two-body interaction (SDI) strength parameters is the transition region. Our strategy of variation parameters is somewhat different from that of Navrátil and Dobesy [16] who vary all the fermion parameters through a prescription laying more stress on the variation of single-particle energies.

It is of course desirable that one should be able to reproduce the observed transition from the same set of parameters used throughout the isotopic chain. It is possible that the drastic truncation of the shell model space mapped onto the boson space and further approximations in the boson space does not allow the interaction to take its

course and demonstrate the transition. This requires us to adjust the parameters by hand to reproduce the transition. However, it has also been shown in shell model calculations [48] that in order to reproduce the observed spectra for all the nuclei in the s-d shell, the two-body matrix elements have to be multiplied by a factor $\sim A^{1/3}$. Such calculations are prohibitively difficult for the set of nuclei under our consideration. Notwithstanding, we can at the least say that the need to vary fermion parameters may be attributed to the absence of excited bosons (s′, d″, g′, ⋯) which may correspond to nearby minima of the variationally minimized energy surface in our HF calculations. Recently it has indeed been shown [14] that inclusion of these bosons does produce better results for lighter nuclei. It is well-known that angular momentum projected HF band-mixing calculations have been eminently successful in studying various spectroscopic properties of nuclei in different regions of the periodic table [49, 50, 51]. We therefore conjecture that if our HF based procedure can be extended to include these excited bosons it may not be necessary to vary the parameters. In summary, we think that the approach proposed in this paper is the simplest, has close connection with the HF band mixing calculations of nuclei and consequently has a natural way of incorporating s′ d′ g′ bosons.

Acknowledgements

We are deeply indebted to our colleagues V K B Kota and Y Durga Devi for allowing us access to the code SDGIBM1 developed and documented by them and for helping us out with the technicalities of running it. Besides, we benefited greatly from discussions with them. We are also grateful to S P Pandya and V K B Kota for a careful reading of the manuscript and for making many useful comments. Thanks are also due to C R Praharaj, B K Agarwal and A K Rath for providing us with the HF code and teaching us how to run it.

References

[1] A Arima and F Iachello, *Phys. Rev. Lett.* **35**, 1069 (1975)
[2] F Iachello and A Arima, *Interacting boson model* (Cambridge University Press, Cambridge, England, 1987)
[3] R F Casten and D D Warner, *Rev. Mod. Phys.* **60**, 389 (1988)
[4] F Iachello and I Talmi *Rev. Mod. Phys.* **59**, 375 (1987)
[5] A Klein and E R Marshalek, *Rev. Mod. Phys.* **63**, 375 (1991)
[6] T Otsuka, A Arima and F Iachello, *Nucl. Phys.* **A309**, 1 (1978b)
[7] S Pittel, P D Duval and B R Barrett, *Ann. Phys. (N.Y.)* **144**, 168 (1982)
[8] Y K Gambhir, P Ring and P Schuck, *Phys. Rev.* **C25**, 2858 (1992a)
[9] Y K Gambhir, P Ring and P Schuck, *Nucl. Phys.* **A384**, 37 (1982b)
[10] O Scholten, *Phys. Rev.* **C28**, 1783 (1983)
[11] A Van Egmond and K Allaart, *Nucl, Phys.* **A425**, 275 (1984)
[12] C H Druce, S Pittel, B R Barrett and P D Duval, *Ann. Phys.* **176**, 114 (1987)
[13] L D Skouras, P Van Isacker and M A Nagarajan, *Nucl. Phys.* **A516**, 255 (1990)
[14] D Bonatsos, L D Skouras, P Van Isacker and M A Nagarajan, *J. Phys.* **G17**, 1803 (1991)
[15] P Navrátil and J Dobesy, *Nucl. Phys.* **A507**, 340 (1990)
[16] P Navrátil and J Dobesy, *Nucl. Phys.* **A533**, 223 (1991)
[17] S Sarangi and J C Parikh, *Pramana - J. Phys.* **40**, 43 (1993)
[18] A Sethi, F Todd Baker, G T Emery, W P Jones and M A Grimm, *Nucl. Phys.* **A518**, 536 (1990)
[19] A Sethi, N M Hintz, D N Mihailidis, A M Mack, M Gazzaly, K W Jones, G Pauletta, L Santi and D Goutte, *Phys. Rev.* **C44** , 700 (1991)

[20] W Pannert, P Ring and Y K Gambhir, *Nucl. Phys.* **A443**, 189 (1985)
[21] T Otsuka, A Arima, and N Yoshinaga, *Phys. Rev. Lett.* **48**, 387 (1982)
[22] D R Bes, R A Broglia, E Maglione, and A Vitturi, *Phys. Rev. Lett.* **48**, 1001 (1982)
[23] N Yoshinaga, A Arima and T Otsuka, *Phys. Lett.* **B143**, 5 (1984)
[24] W Frank and P O Lipas, *J. Phys.* **G16**, 1653 (1990)
[25] Y D Devi and V K B Kota, FORTRAN *programmes for spectroscopic calculations in (sdg)-boson space: The package SDG-IBM1* (PRL-TN-90-68, 1990)
[26] K Allaart, E Boeker, G Bonsignori, M Savoia and Y K Gambhir, *Phys Rep.* **169**, 209 (1988)
[27] S Pittel and J Dukelsky, *Phys. Lett.* **B128**, 9 (1983)
[28] E Cheifetz, R C Jared, S G Thompson and J B Wilhelmy, *Phys. Rev. Lett.* **25**, 38 (1970)
[29] F K Whon, H Mach, M Moszyński, R L Gill and R F Casten, *Nucl. Phys.* **A507**, 141c (1990)
[30] M Liang, H Ohm, B De Sitter, K Sistemich, B Fazekas and G Molnár, *Z. Phys.* **A340**, 223 (1991)
[31] C M Lederer and V S Shirley, (eds) *Tables of isotopes* (Seventh Ed.) (John Wiley, 1978)
[32] S Raman, C H Malarkey, W T Milner, C W Nestor and P H Stelson, *At. Data Nucl. Data Tables* **36**, 1 (1987)
[33] J B French, *in Multipole and sum rule methods in spectroscopy, Proc. Int. School of Physics.* Enrico Fermi, Course 36, Varenna, 1965, edited by C Bloch (Academic Press, New York, 1966) p. 278
[34] P Ring and P Schuck, in *The nuclear many-body problem* (Springer-Verlag, New York. 1980)
[35] P O Lipas, P Von Brentano and A Gelberg, *Rep. Prog. Phys.* **53**, 1355 (1990)
[36] F Iachello, G Puddu, O Scholten, A Arima and T Otsuka, *Phys, Lett.* **B89**, 1 (1979)
[37] W Frank, P von Brentano, A Gelberg and H Harter, *Phys. Rev.* **C38**, 2358 (1988)
[38] Y D Devi and V K B Kota, *Phys. Rev.* **C45**, 2238 (1992)
[39] K Kumar, *Nucl. Phys.* **A231**, 189 (1974)
[40] S K Khosa, P N Tripathi and S K Sharma, *Phys. Lett.* **B119**, 257 (1982)
[41] P Federman and S Pittel, *Phys. Lett.* **B77**, 29 (1978)
[42] H Mach, F K Wohn, G Molnár, K Sistemich, John C Mill, M Moszyński, R L Gill, W Krips and D S Brenner, Nucl. Phys. **A 523**, 197 (1991)
[43] P Federman and S Pittel, *Phys. Lett.* **B69**, 385 (1977)
[44] A de Shalit and M Goldhaber, *Phys. Rev.* **92**, 1211 (1953)
[45] H C Wu, *Phys. Lett.* **B110**, 1 (1981)
[46] M Sambataro and G Molnár. *Nucl. Phys.* **A376**, 201 (1982)
[47] O Scholten, F Iachello and A Arima, *Ann. Phys. (N.Y.)* **115**, 325 (1978)
[48] B H Wildenthal, *Prog. Part. Nucl. Phys.* **11**, 5 (1984)
[49] C R Praharaj and S B Khadkikar, *Phys. Rev. Lett.* **50**, 1254 (1983)
[50] A K Rath, Ph. D Thesis, (Institute of Physics, Bhubaneswar, 1991), unpublished
[51] R Sahu and S P Pandya, *Nucl. Phys.* **A529**, 20 (1991)